NiFe LDH@Super P Nanocomposite as an Efficient Electrocatalyst for Oxygen Evolution Reaction

Li Ren[1], Jiaqi Wang[1], Bing Xue* and Fangfei Li*

Key laboratory of Automobile Materials of Ministry of Education, College of Materials Science and Engineering, Jilin University, Changchun 130025, China.
[1] These authors contributed equally to this work.

Abstract. NiFe LDH (Layered Double Hydroxide) is a promising electrocatalyst for oxygen release reaction (OER), which is currently receiving more and more attention. Here, we propose a simple method to enhance the OER activity of NiFe LDH supported on Super P. The NiFe LDH@Super P catalyst with a nanoflower nanostructure was successfully synthesized via pre-hydrothermal treatment method, which ensures the normal nucleation process of the highly active NiFe LDH precursor and significantly promote the full contact of NiFe LDH and Super P in the three-dimensional space. The as synthesized NiFe LDH@Super P-2h sample exhibited excellent OER performances in alkaline media, and the overpotential is only 260 mV at a current density of 10 $mA \cdot cm^{-2}$. The outstanding OER electrocatalytic reaction performance is attributed to the unique three-dimensional nanoflower structure and excellent composite effect with Super P, which provides more specific surface areas and enables efficient transfer of electrons between them. This research work provides a simple and effective method for developing non-precious metal-based OER catalysts to replace expensive precious metal catalysts.

1 Introduction

The problems of environmental pollution and energy shortage are becoming increasingly prominent and urgently need to be resolved. Specifically, hydrogen is regarded as one of the most promising sustainable energy sources to replace traditional fossil fuels due to its high energy density and environmental friendliness[1]. In recent years, electrocatalytic water splitting has been recognized as a simple and effective technology that can produce clean hydrogen on a large scale [2]. OER that occurs on the anode is considered to be the rate determining step of water electrolysis due to its slow kinetics. It urgently needs an efficient electrocatalyst to accelerate OER at a relatively low overpotential (η) to improve energy conversion efficiency[3]. At present, it is reported that transition metal oxides/hydroxides, especially NiFe layered double hydroxides (NiFe LDHs) are the most active OER catalysts in alkaline environments[4-6].

As we all know, NiFe LDHs has a two-dimensional layered structure, which makes it have a large specific surface area and can expose more catalytically active sites., thus greatly improving the catalytic activity. However, because the nano-sized NiFe LDH easily forms agglomerates, the specific surface area and the number of exposed active sites are reduced, thereby reducing the catalytic performance. In addition, the conductivity of NiFe LDH itself is poor, which is not conducive to electron transfer and also leads to a decrease in catalytic activity[7]. There have been works using highly conductive carbon materials as the substrate to support NiFe LDH nanosheets to try to solve the problems of agglomeration and poor conductivity. However, if the hydrothermal method is used to directly contact the carbon material with the nickel source and the iron source, this will easily affect the nucleation process and crystallinity of NiFe LDH, and the phenomenon of nanoplate agglomeration and the problem of low fixation strength cannot be solved well.

Therefore, this work proposes a stepwise hydrothermal treatment method to prepare a highly active NiFe LDH@Super P composite OER catalyst. First, obtain the NiFe LDH precursor through pre-hydrothermal treatment to ensure the normal nucleation process of the highly active NiFe LDH; then adding Super P for secondary hydrothermal treatment, the active precursor will grow uniformly in situ on the Super P conductive substrate. This process can significantly promote the full contact of NiFe LDH and Super P in the three-dimensional space, which not only greatly increases the load, but also enables efficient transfer of electrons between them, thus significantly improving the conductivity of the catalyst and OER performance.

* Corresponding author: [a]liff@jlu.edu.cn [b]xuebing2011@jlu.edn.cn

2 Experimental

2.1 Synthesis of the NiFe LDH@Super P

All chemicals are analytically pure and can be used directly after purchase without further purification. NiFe LDH@Super P with Ni:Fe ratio of 2:1 was synthesized using a steped hydrothermal method. In a typical procedure, 3.6 mmol of $Ni(NO_3)_2{\cdot}6H_2O$, 1.8 mmol of $Fe(NO_3)_3{\cdot}9H_2O$, 126 mmol of urea and 27 mmol NH_4F were dissolved in 100 ml deionized water at room temperature and stirred to form a homogeneous solution. Then it was transferred to a 100 ml Teflon-lined stainless steel autoclave and kept at 100 °C for a certain period of time. Then 0.05 mg Super P was added to it for the second hydrothermal treatment. After cooling down to room temperature, the resulting powder was collected by centrifugation, washed 5 times with deionized water and dried at 60 °C for 12 h in a vacuum drying oven.

For comparison, the second hydrothermal treatment time were 1 h, 2 h, and 3 h, respectively. The corresponding powders were labelled as NiFe LDH@Super P-1h, NiFe LDH@Super P-2h, NiFe LDH@Super P-3h. In addition, in order to serve as a comparative sample, NiFe LDH@Super P is also directly synthesized by one-step hydrothermal method, that is, 0.05 mg Super P is added to the mixed solution before the hydrothermal treatment, and it is named NiFe LDH@Super P-1.

2.2 Characterization

The X-ray diffraction (XRD) of the sample was characterized by an X-ray diffractometer (DX-2700) at 35 kV and 25 mA using CuKα radiation (λ = 1.5418 Å). A specific surface area and pore size analyzer (JW-BK222, China) was used to perform the N_2 adsorption-desorption isotherm. Use field emission scanning electron microscope (JSM-6700F) to characterize the micro morphology of the sample.

2.3 Oxygen evolution reaction (OER) tests and electrochemical measurements

The electrochemical measurement was performed on a CHI604E electrochemical workstation with a standard three-electrode system. 1 M KOH solution was used as the electrolyte. The counter electrode is a Pt wire net, and the reference electrode is a Hg / HgO electrode. A glass carbon electrode (GCE) with a diameter of 3 mm was used as the working electrode. All test patterns are corrected by ohmic compensation. Cyclic voltammetry curves (CVs) were performed between 1.0 and 1.7 V vs. RHE at a scan rate of 100 $mV{\cdot}s^{-1}$. Linear sweep voltammetry (LSV) measurements were recorded from 0.2-0.8 V vs. Hg/HgO with a scan rate of 10 $mV{\cdot}s^{-1}$ for the polarization curves. The Tafel slopes were obtained by plotting the overpotential (η) against log (j) from LSV curves. Electrochemical impedance spectroscopy (EIS) was performed with an overpotential of 0.3 V in the frequency range of 0.01 to 10^5 Hz.

3 Results and Discuss

The XRD patterns of the materials are illustrated in Figure 1. The diffraction peaks of the samples are indexed to NiFe LDH, agreeing well with the standard powder diffraction patterns (JCPDF no. 40-0215)[8]. Specifically, the characteristic peaks of the (003), (006), (012), (110) and (113) crystal planes of NiFe LDH are located at 11.6°, 23.45°, 34.4°, 59.9° and 61.3° respectively, and the peak shape is sharp, indicating that the crystallinity of the synthesized sample is high. It is worth noting that the typical pattern of Super P cannot be found in the XRD pattern of the NiFe LDH@Super P composite. This may be because the proportion of Super P in the nanocomposite is so low that the peak of NiFe LDH is completely covered the peak of Super P. In addition, the peak intensity of NiFe LDH@Super P-1 is relatively low, possibly because the direct addition of Super P to the mixed solution affects the normal nucleation process of NiFe LDH.

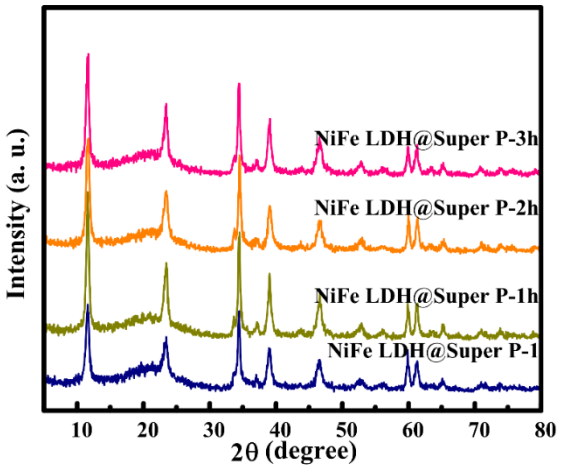

Figure 1. XRD patterns of the samples.

The morphological characteristics of NiFe LDH@Super P synthesized under different conditions were revealed by field emission scanning electron microscope (FESEM). Figure 2a shows the structure of the NiFe LDH@Super P-1. There is fewer NiFe LDH nanoflower formed, and most of the observations are agglomerated carbon particles, which shows that mixing Super P and salt solution directly will have a serious impact on the growth of NiFe LDH. This is also consistent with the XRD analysis results. From Figure 2b, the flower-like NiFe LDH is formed, but the distribution of NiFe LDH nanoflowers is relatively scattered and small in size, which indicates that the precursors in the first stage have not been fully developed. When the pre-hydrothermal time is 2 h (Figure 2c-d), a large number of uniform flower-like microspheres appeared and the thickness of the nanosheet is about 20 nm, which proves that the synthesized NiFe LDH is a nanostructure. At the same time, the NiFe LDH nanoflower is evenly in-situ loaded on Super P. As can be seen from Figure 2e-f, when the pre-hydrothermal time is 3 h, the morphology of NiFe LDH@Super P-3h is almost the same as that of NiFe LDH@Super P-2h. When the pre-hydrothermal treatment time reaches 2 hours, the precursor of NiFe LDH will continue to grow and be perfect during the second

hydrothermal treatment, and it can be loaded on Super P very well.

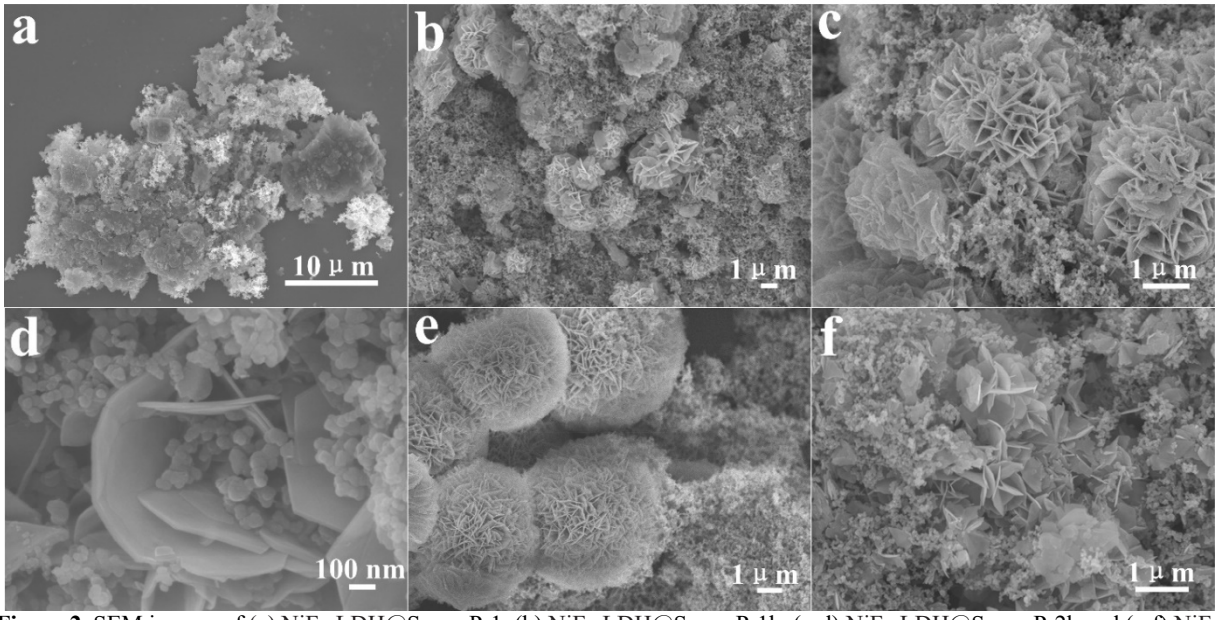

Figure 2. SEM images of (a) NiFe LDH@Super P-1, (b) NiFe LDH@Super P-1h, (c-d) NiFe LDH@Super P-2h and (e-f) NiFe LDH@Super P-3h.

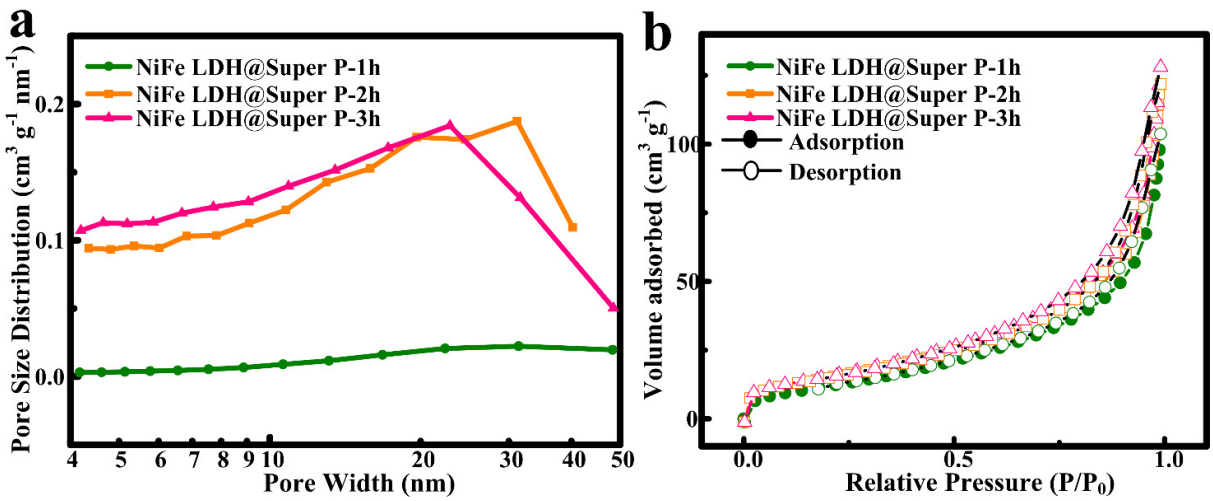

Figure 3. (a) Pore size distribution and (b) N_2 adsorption-desorption isotherm curves of the samples.

The pore structure and specific surface area of all samples synthesized under different hydrothermal conditions were determined by low-temperature nitrogen adsorption/desorption measurements. It can be seen from Figure 3 that all isotherms are shown as typical type IV with H3 hysteresis loop, which is in good agreement with previous reports[9]. The size distribution (Figure 3a) exhibits an average pore size of 15-30 nm. Moreover, the specific surface areas of NiFe LDH@Super P-1h, NiFe LDH@Super P-2h and NiFe LDH@Super P-3h are 49.88, 60.283 and 61.989 $m^2 \cdot g^{-1}$, respectively. The smaller specific surface area of NiFe LDH@Super P-1h may be due to the fact that NiFe LDH nanoflower has not been formed in large quantities. However, these relatively large specific surface areas and mesoporous channels will expose more active sites, which will further lead to faster penetration of electrolyte and rapid diffusion of molecular oxygen during the OER process[10].

The as-prepared electrocatalysts were systematically evaluated for oxygen evolution reaction (OER). Figure 4a presents the linear sweep voltammograms (LSV) curves of all samples, which clearly shows that the NiFe LDH@Super P-2h sample exhibits the smallest overpotential of 260 mV at the current density of 10 $mA \cdot cm^{-2}$ and the earliest onset of potential compared with the other samples. Obviously, the polarization curve of the NiFe LDH@Super P-1 sample is the worst, and its η10 is 20 mV higher than that of NiFe LDH@Super P-2h. Tafel slope is also a useful parameter to describe the kinetics of water electrolysis. The Tafel diagram (Figure 4b) obtained from the polarization curve of each NiFe LDH@Super P also shows that the NiFe LDH@Super P-2h sample has the lowest Tafel slope of 24.81 $mV \cdot dec^{-1}$, which further indicates its highest intrinsic catalytic activity among them[11]. The predictable maximum tafel slope of NiFe LDH@Super P-1 sample is 48.92 $mV \cdot dec^{-1}$. It can be seen

from Figure 4c that the resistance of the catalysts can be greatly reduced after the pre-hydrothermal treatment, which also shows that Super P as a carrier can greatly enhance the conductivity. In practical applications, the long-term durability of catalytic electrodes is another key issue to be considered, especially for these nanostructured films, whether they have good durability determines whether they have practical value. We examined the stability of the most catalytically active NiFe LDH@Super P-2h sample for OER. After a long-term cycle of 3000 cycles at a scan rate of 100 $mV \cdot s^{-1}$, its polarization curve is almost the same as the initial one, and the current density loss is negligible (Figure 4d), which confirms the working stability of the electrode. In addition, the cycle stability of other catalysts was also tested. The cycle stability performance of NiFe LDH@Super P-1 is relatively poor. As the cycle time increases, its overpotential also gradually increases, especially at higher current density, which may be due to the weak bond between NiFe LDH and Super P. This shows that the synthesis process of pre-hydrothermal treatment and then adding Super P as a support has a significant effect on the improvement of OER catalytic performance.

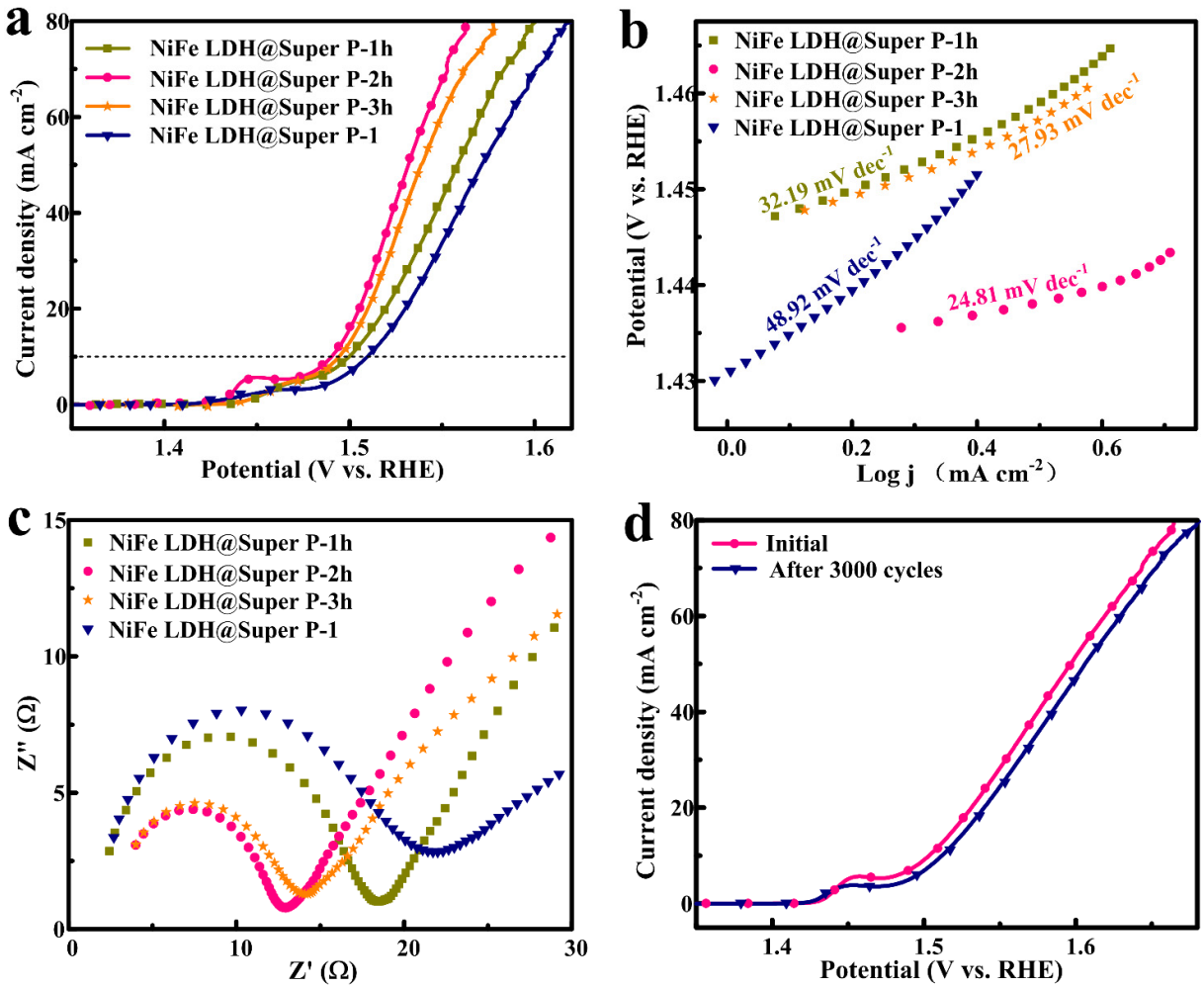

Figure 4. Electrocatalytic OER performances of the samples. (a) LSV polarization curves, (b) Tafel plots, (c) Electrochemical impedance spectras and (d) LSV curves of NiFe LDH@Super P-2h before and after cycling tests.

4 Conclusion

In summary, the NiFe LDH@Super P catalysts were fabricated by pre-hydrothermal treatment method. The as synthesized NiFe LDH@Super P-2h sample exhibited excellent OER performances in alkaline media, with an overpotential of only 260 mV at the current density of 10 $mA \cdot cm^{-2}$. Moreover, after long-term CV cycle measurement, the performance loss of the material is almost negligible, and it can still maintain very high electrocatalytic activity. The excellent OER electrocatalytic performance is mainly attributed to its unique three-dimensional nanoflower structure and excellent compounding effect with Super P, which could expose more active sites and provide a more convenient way of charge/mass transfer, thus speeding up the OER electrochemical reaction kinetics. This study affords a facile and cost effectively strategy to realize the best performance of OER catalysts, which will provide an effective way to rationally design other transition metal LDHs electrocatalysts suitable for a wide range of technical applications.

References

1. Seh, Z. W.; Kibsgaard, J.; Dickens, C. F.; Chorkendorff, I.; Norskov, J. K.; Jaramillo, T. F. Science. 355, eaad4998 (2017)
2. Wang, JH.; Cui, W.; Liu, Q.; Xing, ZC.; Asiri, AM.; Sun, XP. Adv. Mater. 28, 215-230 (2016)
3. Suen, N. T.; Hung, S. F.; Quan, Q.; Zhang, N.; Xu, Y. J.; Chen, H. M. Electrocatalysis for the oxygen evolution reaction: recent development and future perspectives. Chem. Soc. Rev. 46, 337–365 (2017)
4. Kuai, CG.; Zhang, Y.; Wu, DY.; Sokaras, D.; Mu, LQ.; Spence, S.; Nordlund, D.; Lin, F.; Du, XW. ACS Catal. 9, 6027–6032 (2019)
5. Lu, ZY.; Xu, WW.; Zhu, W.; Yang, Q.; Lei, XD.; Liu, JF.; Li, YP.; Sun, XM.; Duan, X. ChemComm. 50, 6479–6482 (2019)
6. Gao, ZW.; Liu, JY.; Chen, XM.; Zheng, XL.; Mao, J.; Liu, H.; Ma, T.; Li, L.; Wang, WC.; Du, XW. Adv. Mater. 2019, 31, 1804769 (2019)
7. Ni, YM.; Yao, LH.; Wang, Y.; Liu, B.; Cao, MH.; Hu, CW. Nanoscale. 9, 11596–11604 (2017)
8. .Shen, J.; Zhang, P.; Xie, RS.; Chen, L.; Li, MT.; Li, JP.; Ji, BQ.; Hu, ZY.; Li, JJ.; Song, LX.; Wu, YP.; Zhao, XL. ACS Appl. Mater. Interfaces. 11, 13545–13556 (2019)
9. Li, X.; Fan, ML.; Wei, DN.; Wang, XL.; Wang, YL. J. Electrochem. Soc. 167, 024501 (2020)
10. Zhan, TR.; Zhang, YM.; Liu, XL.; Lu, SS.; Hou, WG. J. Power Sources. 333, 53–60 (2016)
11. Peng, CL.; Ran, N.; Wan, G.; Zhao, WP.; Kuang, ZY.; Lu, Z.; Sun, CJ.; Liu, JJ.; Wang, LZ.; Chen, HR. ChemSusChem. 13, 811–818 (2020)